

EVALUATION OF FULL SCALE EMBANKMENT WITH HEXAGONAL WIRE MESH REINFORCEMENT WITH ADDITIONAL SURCHARGE

P. Voottipruex¹ and D.T. Bergado²

ABSTRACT

A fully instrumented test embankment reinforced with hexagonal wire mesh was constructed on soft clay foundation in Thailand. The reinforced wall consisted of 90 degrees inclined gabion facing on one side and a sloping unreinforced sandfill in the opposite side with a total height of 6.0 meters. The existing embankment was later raised up to another 1.0 m. The maximum observed settlement and lateral movement due to additional surcharge was 0.049 m at 190 days and 0.007 m at 173 days, respectively. The excess pore pressure increased due to additional surcharge and gradually dissipated. The predicted settlement by using C_v from Asaoka's method presents a higher rate of settlement than by using C_v from oedometer test. The calculated settlement by Asaoka's method is closer to the observed settlement. The maximum tension lines in the test embankment were closer to the tie-back wedge assumption. The tension induced in the hexagonal wire mesh in the laboratory during pullout test was higher than the monitored data from the full scale embankment wherein the tension induced in the zinc-coated hexagonal wire mesh was slightly higher than the PVC-coated. The forces developed in the reinforcement of full scale embankment was in the working stress level where the corresponding laboratory pullout tension and displacement of reinforcement in the field were correlated. The external stability of the test embankment has been verified to be safe.

INTRODUCTION

A gabion facing structure can be modified into a reinforced wall/embankment system by adding a hexagonal wire mesh reinforcement anchor to its backfill. The first structure with gabion facing and anchored to the backfill with steel strips was built in Sabah, Malaysia in 1979 (Macaferti, 1990). Lo (1990) and Lo and Li (1990) conducted pullout tests to determine the design parameters of hexagonal wire mesh. A series of large scale laboratory tests were conducted to measure the pull-out resistance and load-elongation response of the reinforcing mesh panels when embedded in a granular soil. The test results unambiguously establish significant increases, compared to uniaxial testing in air, in both strength and stiffness values of a mesh panel due to embedment in granular soil subject to overburden stress. Indraratna and Lasek (1996) evaluated the load-deflection behavior of clay beams reinforced with galvanized wire netting. The use of galvanized steel wire netting as reinforcement in the tensile zone of the beams provides a substantial increase in flexural tensile, and enables the beams to sustain much larger deformations without causing complete failure. Moreover, the reinforced clay beams demonstrate a definite ductile-plastic (post-peak) behavior following the pre-peak elasto-plastic response. Mir (1996) conducted in-air tensile and pullout tests of hexagonal wires and possible applications were explored (Bergado et al, 1998a). The two types of hexagonal wire mesh tested were the Camel Brand of B.B. Trading (Malaysia): one is zinc-coated while the other is zinc-coated with PVC sleeve. Further pullout tests using different backfill materials were conducted (Kabiling, 1997; Bergado et al, 1998b). Teerawatanasuk (1997) conducted direct shear tests and further interaction studies. Moreover, field and laboratory pullout tests were conducted to obtain data on the interaction and pullout mechanism of the wire mesh with silty sand backfill (Wongsawanon, 1998; Modmoltin, 1998). A 6 m fully instrumented reinforced embankment was constructed and monitored to investigate the field behavior of gabion facing embankment with hexagonal wire mesh embankment (Voottipruex et al, 1998; Khwanpruk, 1998) Finally, the embankment was raised up to another 1 m and was monitored and analyzed (Anujorn, 1999). This paper is concerned with the deformation characteristics of the hexagonal wire mesh reinforcement of a reinforce wall/embankment system based on field monitored data before and after additional surcharge load.

¹ Doctoral Candidate, School of Civil Engineering, Asian Institute of Technology, P.O.Box 4, Klong Luang, Patumthani 12120, Thailand
² Professor of Geotechnical Engineering, School of Civil Engineering, Asian Institute of Technology, P.O. Box 4, Klong Luang, Patumthani 12120, Thailand

Note: Discussion is open until 1 August 2000. This paper is part of the *Geotechnical Engineering Journal*, Vol. 30, No. 3, December 1999. Published by the Southeast Asian Geotechnical Society, ISSN 0046-5828.

HEXAGONAL WIRE MESH EMBANKMENT WITH GABION FACING

The hexagonal wire mesh embankment was constructed inside the campus of the Asian Institute of Technology (AIT) located 42 kms north of Bangkok, Thailand. The cross-sectional view of the test embankment is shown in Fig. 1. The soil profile and properties are plotted down to 10.0 m depth as shown in Fig. 2. The uppermost soil profile can be divided into 3 sublayers, namely: weathered crust, soft clay and stiff clay. The weathered crust consisting of heavily overconsolidated reddish-brown clay forms the uppermost 2 m thick layer followed by grayish soft clay layer about 6 m thick. The soft clay layer is underlain by stiff clay found at 8.0 to 15.0 m depth. Below the stiff clay layer is the dense sand layer of more than 10.0 m thick.

The plan and cross-section as well as the instrumentation layout of the test embankment are shown in Fig. 3. There are three surface settlement plates for each type of hexagonal wire mesh reinforcement and 2 subsurface settlement plates at 3 m and 6 m depths. Open standpipe piezometers and inclinometers were provided to monitor the pore pressures and the lateral movements of the embankment, respectively.

The construction of the wall involved the placement of the gabion facing unit with reinforcement attachment at every 0.5 m vertical spacing. The gabion facing was first filled with boulder. After placing the gabion wall filled with boulder, the first reinforcement was placed and instrumented. The backfill was spread out in 0.15 m lifts to a total of 0.5 m with the required density of 95% of standard Proctor and compacted with combination of roller compactor and wherein the settlement plate, standpipe piezometer and inclinometer were installed. After completion, the embankment with hexagonal wire mesh reinforcement was 6.0 m high, 6.0 m long, and 6.0 m at the top with a base width of 18.0 m. The embankment was divided into two sections along its length (see Fig.3). Each sections was constructed using different type of hexagonal wire mesh, namely: zinc-coated and PVC-coated using the same backfill material. The inclination of the gabion facing wall was 90 degrees from the horizontal. The side slope and back slope have an inclination of 1 vertical to 1 horizontal inclination.

Additional surcharge of 1 meter high was constructed on top of the existing hexagonal wire mesh embankment. One thousand plastic sand bags each filled with 40 kgs of Ayutthaya sand were laid in one cubic meter of gabion cage. Thus, the unit weights of additional surcharge load amounted to 16.7 kN/m². To prevent degradation of sandbags from ultraviolet rays, geotextiles were used to totally cover the plastic sand bag. The existing embankment with additional surcharge is shown in Fig. 4.

UNDRAINED SHEAR STRENGTH

The undrained strength parameters were obtained by Anujorn (1999) and Khwanpruk (1998) using UU and UC tests and are plotted with depth as shown in Fig. 5. From the test results, the lowest strength was found at 3.0 to 4.5 m depth below the ground surface. It can be observed that the undrained strength values from UU test are slightly higher than the undrained strength from UC. This is due to the presence of confining stress in the UU test. The confining stress in the UU test closed the fissures and shear resistance developed, hence, higher shear strength was obtained.

MAXIMUM PAST PRESSURE

The preconsolidation pressure is the maximum pressure to which the soil has been subjected throughout its geologic history. It represents a yield stress that separates small strain "elastic" behavior from large strain "plastic deformation" during one-dimensional compression. The preconsolidation pressure of each layer are tabulated in Table 1. These values were obtained using the empirical method of Casagrande (1936). The void ratio versus effective stress in logarithmic scale are plotted in Fig. 6. In this case, the value of preconsolidation pressure ranges from 85 to 100 kPa. The values of overconsolidated ratio (OCR) of the subsoil prior to embankment construction and one year after embankment construction are also summarized in Table 1. One year after construction, the effective stress in the subsoil changed due to embankment load with stress increment of 108 kPa. At this stage, the effective stress of the subsoil exceeded the maximum past pressure which reduced the overconsolidation ratio to one in some layers. Therefore, during application of the additional surcharge, the subsoil is in normally consolidated state.

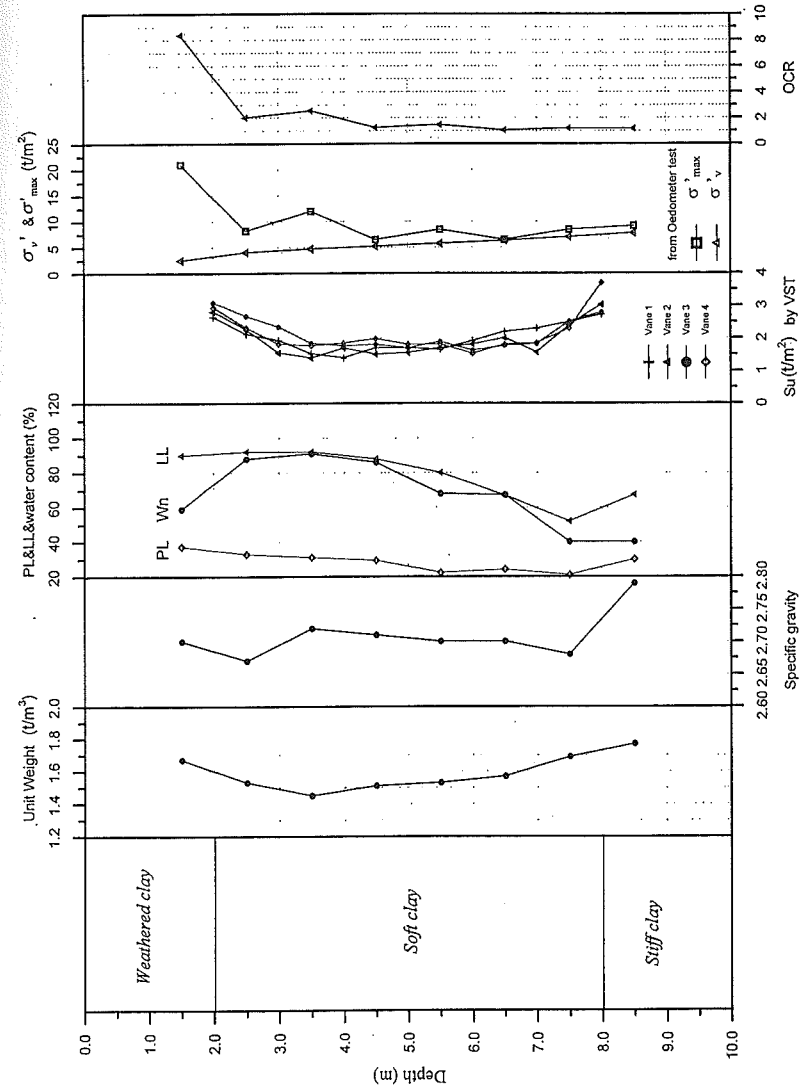


Fig. 1 Soil Profile and Properties

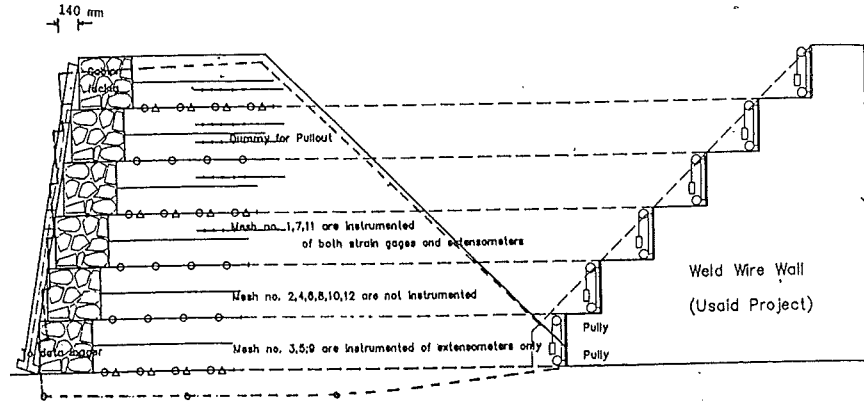


Fig. 2 Hexagonal Wire Mesh Embankment

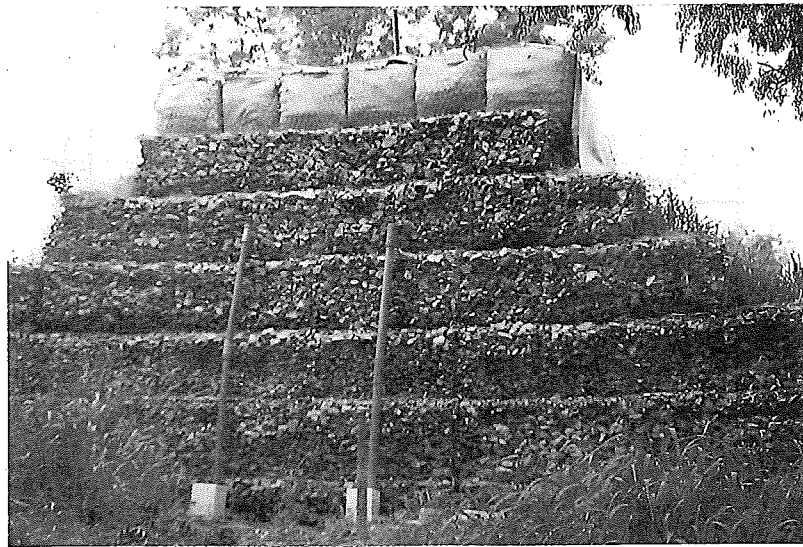


Fig. 3 Additional Surcharge Laid on the Existing Embankment

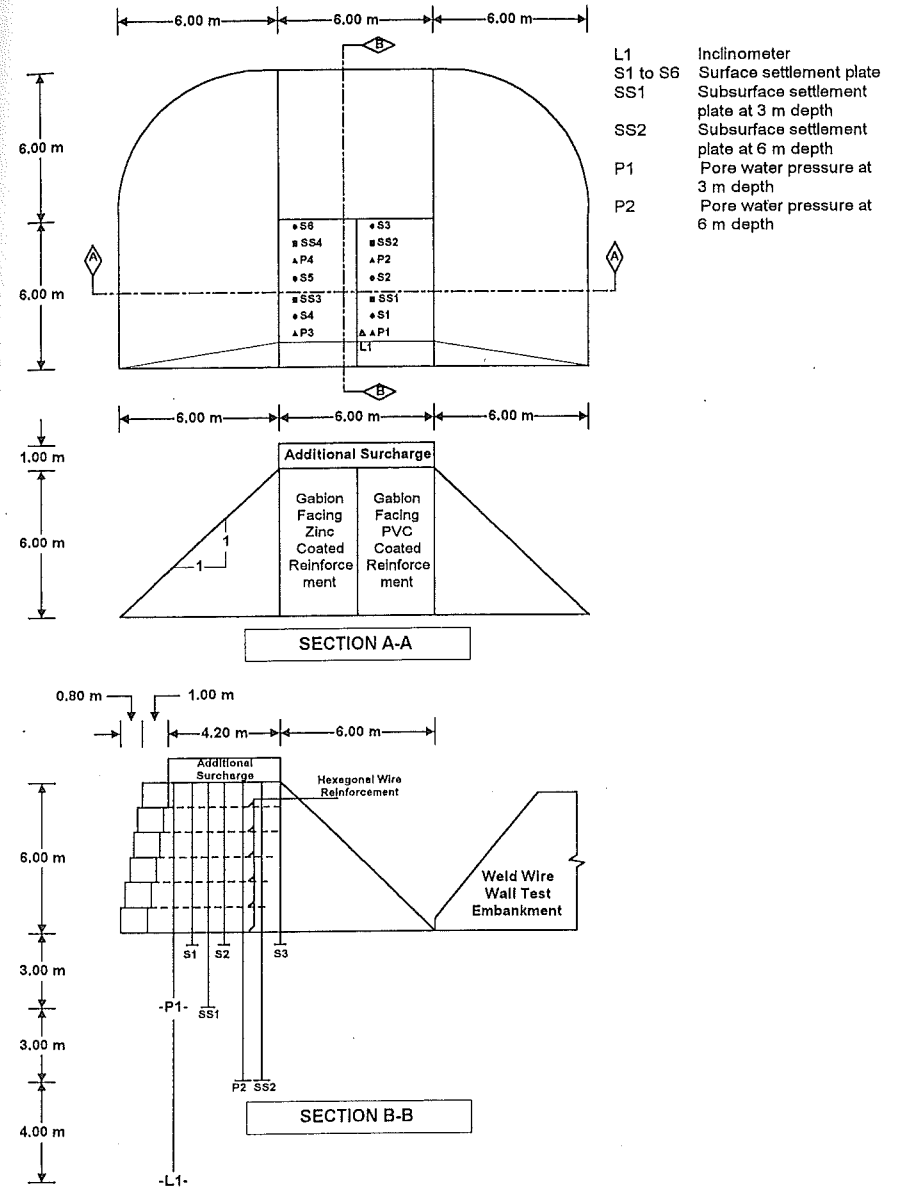


Fig. 4 The Plan and Cross-Section of Monitoring Instrumentations

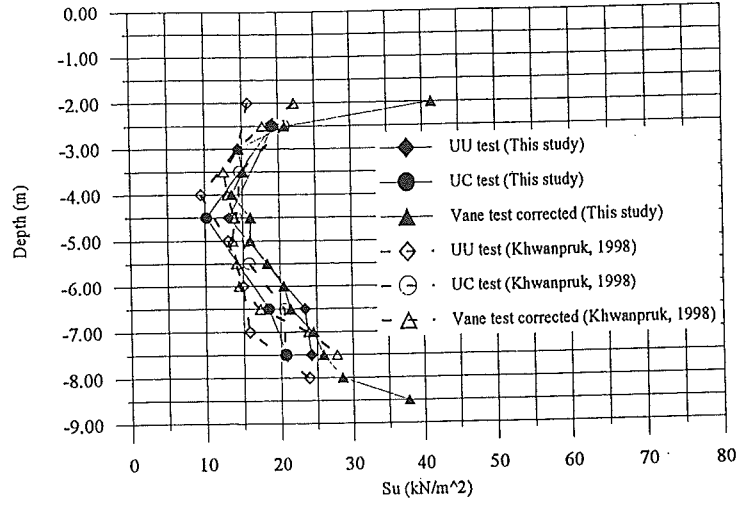


Fig. 5 Undrained Strength Versus Depth of Various Testing

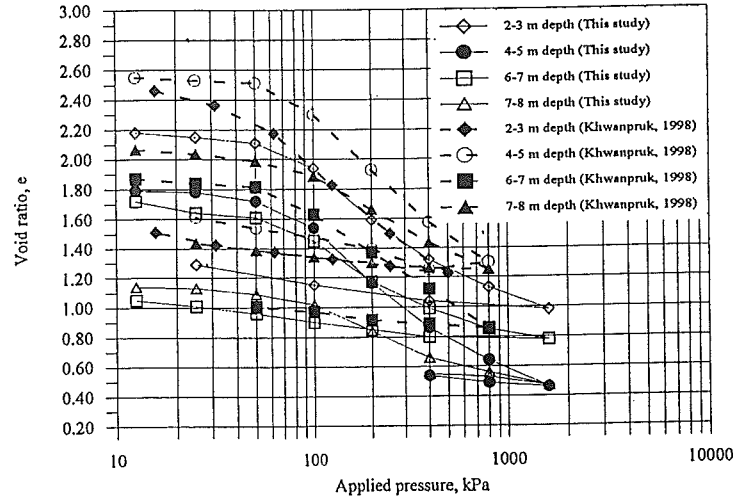


Fig. 6 Void Ratio Versus Applied Pressure at Various Depth from Oedometer Test

Table 1 General Properties of Soil at the Site

Depth m	γ_t kN/m ³	W_n %	G_s	e_0	PL %	LL %	PI %	LI %	S_u kPa	u kPa	σ_{vo} kPa	σ'_{vo} kPa	$\Delta\sigma'_{vo}$ kPa	σ'_{vc} kPa	σ'_{max} kPa	OCR
2.5	12.85	60.89	2.74	2.43	32.61	84.6	51.99	0.54	20.82	15.0	32.13	17.13	77.82	95.0	86.7	1.00
4.5	15.97	90.91	2.66	2.18	34.35	100.8	66.45	0.85	16.06	35.0	64.07	29.07	64.48	93.5	91.5	1.00
6.5	15.28	52.78	2.59	1.59	27.23	67.32	40.09	0.76	20.4	55.0	94.63	39.63	55.76	95.4	85.7	1.00
7.5	17.39	38.23	2.63	1.09	28.01	61.75	33.74	0.30	25.9	65.0	112.02	47.02	52.2	99.2	95.2	1.00

Ground water level is located at -1.00 m (July, 1997)

σ'_{vo} = original effective stress

$\Delta\sigma'_{vo}$ = due to pressure is applied by embankment

Table 2 Calculation of Settlement by Using Data from Oedometer Test Due to Additional Surcharge

No. of Layer	Thickness H (m)	e_0	W %	C_r	C_c	$H/(1+e_0)$	σ'_{vo}	σ'_p	OCR*	$\Delta\sigma'_v$	μ	P_{1-D}	P_{3-D}
1	2.5	2.43	60.89	0.114	1.07	107.36	107.36	107.36	1.00	15.60	0.75	0.046	0.034
2	2	2.18	90.91	0.049	1.02	93.09	93.10	93.10	1.00	11.60	0.95	0.033	0.031
3	2	1.59	52.98	0.098	0.56	93.44	93.44	93.44	1.00	10.00	0.96	0.019	0.018
4	1.5	1.09	38.23	0.033	0.66	97.77	97.80	97.80	1.00	8.14	0.97	0.016	0.016
Total												0.114	0.100

Remark: water table was located at -1.00 m depth below general ground surface

σ'_{vo} = initial stress + stress applied by embankment

$\Delta\sigma'_v$ = stress applied by additional surcharge

OCR* = 1.00 due to the effective stress over the max past pressure

Table 3 Calculation of Settlement by Using Water Content Method due to Additional Surcharge

$C_c = 0.0129w + 0.009$, $\sigma'_p = -0.1831w + 96.299$, $C_r = 0.0018w + 0.1868$

No. of Layer	Thickness H (m)	e_0	W %	C_r	C_c	$H/(1+e_0)$	σ'_{vo}	σ'_p	σ'_v	OCR**	$\Delta\sigma'_v$	ρ (m)
1	2.5	2.43	60.89	0.114	1.07	0.73	107.36	107.36	107.36	1.00	15.60	0.034
2	2	2.18	90.91	0.049	1.02	0.63	93.09	93.10	93.10	1.00	11.60	0.038
3	2	1.59	52.98	0.098	0.56	0.77	93.44	93.44	93.44	1.00	10.00	0.024
4	1.5	1.09	38.23	0.033	0.66	0.72	97.77	97.80	97.80	1.00	8.14	0.013
Total												0.108

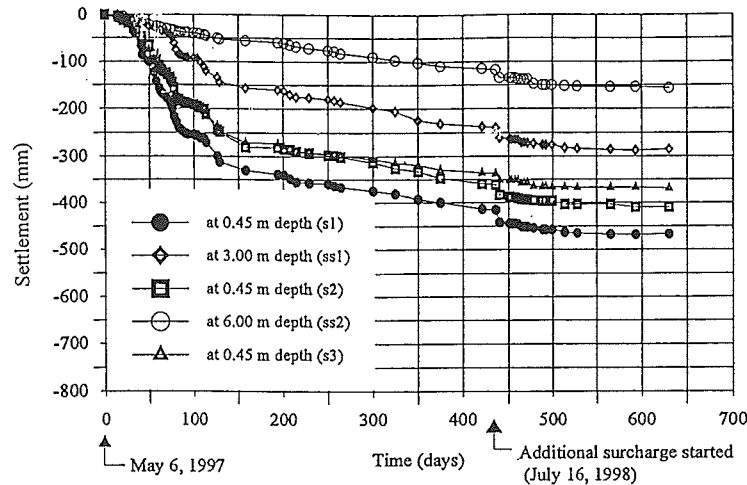


Fig. 7 Settlement Versus Time of Test Embankment at Zinc-Coated Area

OBSERVED SETTLEMENT

Before and after the installation of additional surcharge, the surface and subsurface settlements beneath the embankment were observed by the surface settlement plates and subsurface settlement gages, respectively. Figure 7 shows the plot of the surface settlements from plates S1 to S6 and Fig. 8 shows the subsurface settlements from gages SS1 to SS4 for both PVC-coated and zinc-coated hexagonal wire mesh reinforcements. The surface settlement at S1 represent the maximum settlement of 40 mm before installation of additional surcharge, additional settlement of 17 mm after the end of additional surcharge construction, and 49 mm after

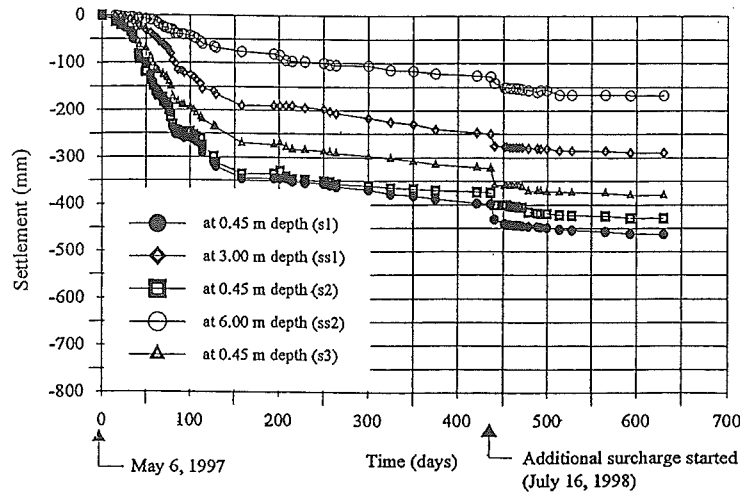


Fig. 8 Settlement Versus Time of Test Embankment at PVC-Coated Area

190 days since the beginning of construction of surcharge. The degree of consolidation is about 80%. The subsurface settlement gages at 3.0 m and 6.0 m were slightly different. Most of the surface and subsurface settlement slowly increased after about 50 days since the beginning of construction of surcharge.

The maximum surface settlement after construction of embankment including the additional surcharge was about 435.5 mm occurring at the front face of embankment (S4) after about 630 days since the beginning of embankment construction. The subsurface settlement showed the maximum settlement at about 278 mm and 164 mm at SS1 and SS2, respectively.

The settlement profile of the subsoil below the reinforced embankment was plotted to compare with the settlement profiles below the reinforced soil mass of the steel grid and geogrid reinforced embankments (Alfaro, 1996) as shown in Fig. 9. Larger settlements were observed below the toe than below the center of the embankment especially in the steel grid reinforced wall embankment. The steel grid which is on inextensible reinforcement is capable of acting more as a rigid block than the geogrid which is an extensible reinforcement. In this study, the trend of the settlement profile of hexagonal wire mesh reinforcement seems to be similar to the case of geogrid reinforcement. A more rigid reinforced mass tends to rotate more about the toe due to the lateral thrust from behind.

Figure 10 shows the comparison of toe settlement of the three embankments. The settlement of steel grid embankment is larger than those of the geosynthetic embankment and hexagonal wire mesh embankment. In the case of steel grid and geogrid embankments, the weathered clay crust was first broken along the edges of the embankment system and also at the center, both in longitudinal and in the transverse directions, by excavation of a trench with a width of about 1 foot (0.3 m) to a depth of 2 m below the general ground surface.

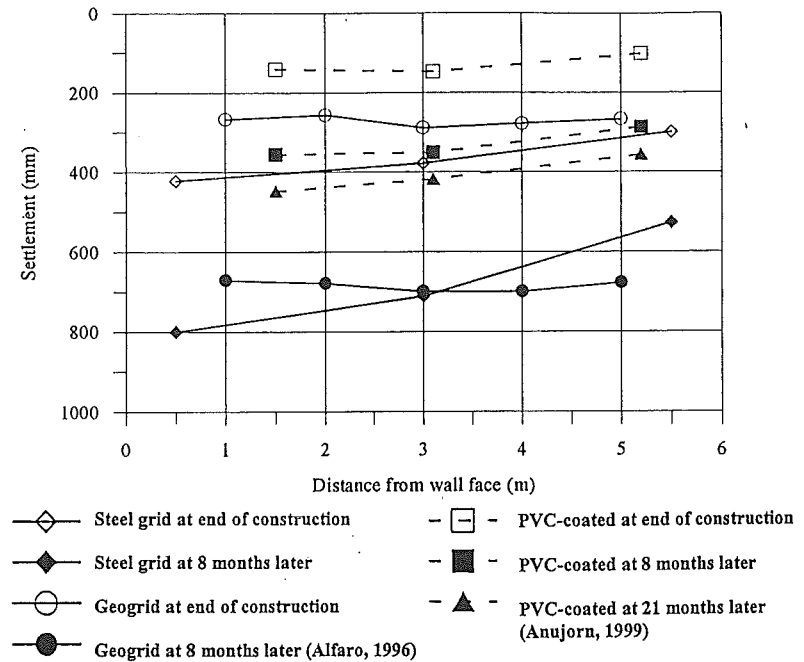


Fig. 9 Settlement Profiles Below Wall/Embankment of Previous Types of Reinforcement at Different Period

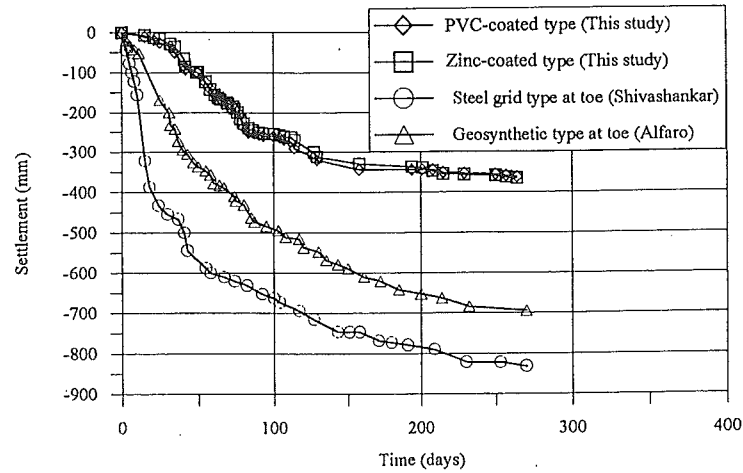


Fig. 10 Comparison of Surface Settlement in the Subsoil at Different Reinforcement Type

The trench was then filled up with the same excavated material and compacted with a hand compactor before placing the first layer of reinforcement. The objective was to eliminate the weathered clay crust beneath the embankment to act as a floating raft foundation. In the hexagonal wire embankment, the weathered clay crust underneath the embankment was not excavated prior to construction. This is the main reason for lower settlement magnitudes than the other two embankments. Moreover, the steel grid embankment behaved as a rigid mass due to inextensible and seem to rotate more which caused larger settlement at the toe than using the geogrid embankment. The geogrid reinforcement is an extensible material and, hence, less rotation occurred than the steel grid embankment.

PORE WATER PRESSURE

The pore water pressures in the soft clay foundation were obtained from two piezometers, located at 3 m and 6 m depth for both types of hexagonal wire mesh reinforcement. The location of the piezometers are shown in Fig. 3. Before surcharge, the pore pressure continued to decline at a very slow rate resulting from the dissipation of excess pore water pressure with time. After the installation of additional surcharge, the pore pressure increased rapidly and slowly decreased afterwards due to very low rate of dissipation and became constant 50 days after the addition of surcharge. The total pore pressures are plotted versus time in Figs. 11 to 12 for PVC-coated and zinc-coated areas, respectively.

Figures 13 and 14 show the pore pressure versus depth at the dummy area and below the embankment, respectively. It can be observed that the hydrostatic pressure fluctuated in each period. The total pore pressure versus depth of the dummy area is plotted for comparison. The water table fluctuated between -0.262 m to -2.071 m from the original ground. The excess pore pressure versus time plot from the beginning of embankment construction until additional surcharge are shown in Figs.15 and 16.

The excess pore pressure depend on Skempton's pore pressure parameter, A_v (which is said to approximate the pore pressure coefficient at failure, A_f), and the geometry of the loading condition (Skempton and Bjerrum, 1957). Lambe (1962) reports that for slightly overconsolidated clays, the value of A_f should be from 0.3 to 0.7. Cox (1968) also reported similar results with Bangkok clay subsoil. The excess pore pressure vary from 50 % of the increase in the vertical stresses for overconsolidated clay to 100 % of the increase in the vertical stresses for normal consolidated clay.

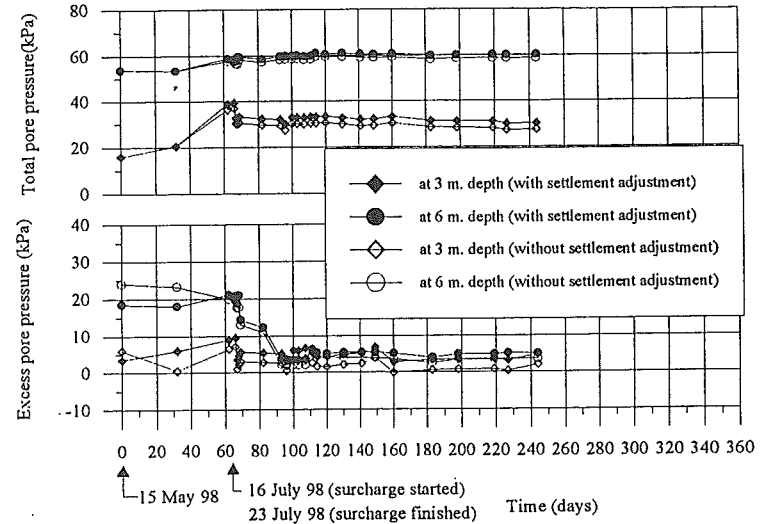


Fig. 11 Total Pore Pressure and Excess Pore Pressure Versus Time Below PVC-Coated Area (at Front)

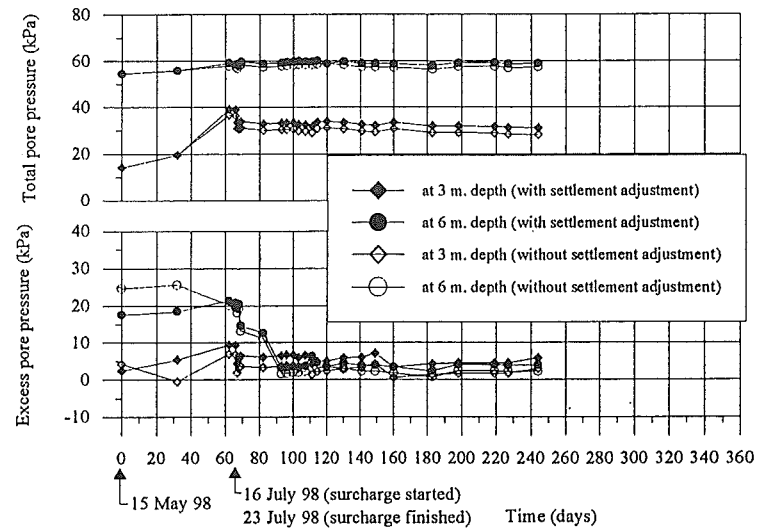


Fig. 12 Total Pore Pressure and Excess Pore Pressure Versus Time Below Zinc-Coated Area (at Front)

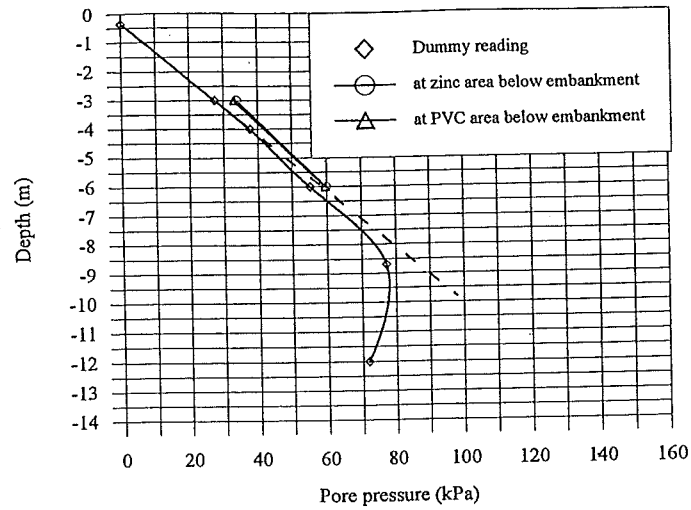


Fig. 13 Pore Pressure Versus Depth on July 23, 1998 (Immediately After Additional Load)

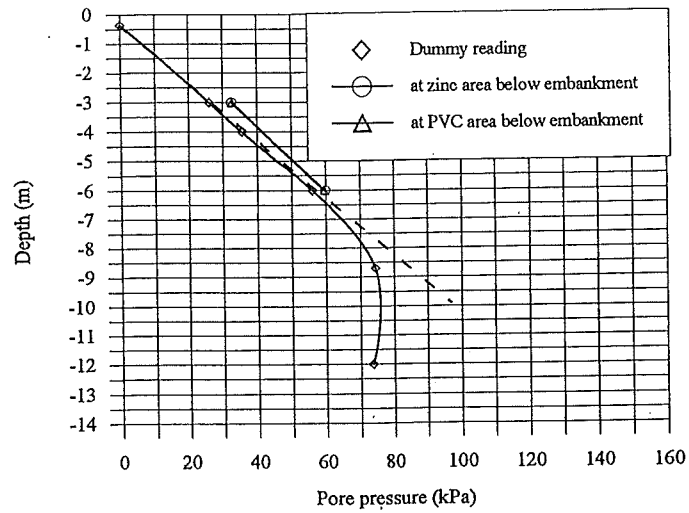


Fig. 14 Pore Pressure Versus Depth on August 28, 1998 (38 Days After Additional Load)

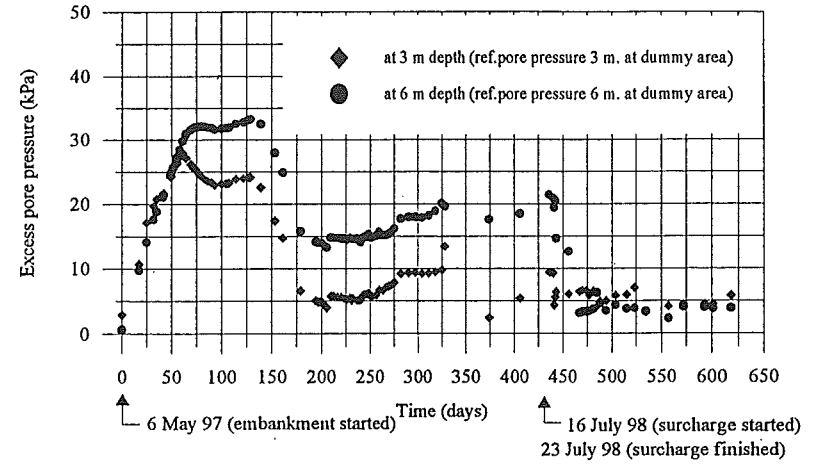


Fig. 15 Excess Pore Pressure Versus Time Underneath Zinc-Coated Area

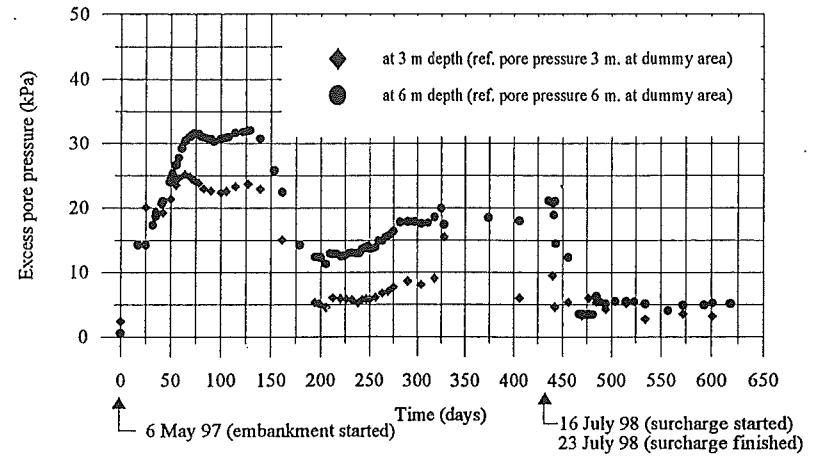


Fig. 16 Excess Pore Pressure Versus Time Underneath PVC-Coated Area

LATERAL MOVEMENT

One inclinometer was installed near the front face of the embankment as shown in Fig. 3. The lateral movement was monitored since 2 July 1997, until additional surcharge was constructed since 16 July 1998. The total monitoring periods are 379 days from starting date. The lateral movement increased significantly until the maximum value within 173 days. Afterwards, the lateral movements decreased. In case of the additional surcharge, the load applied to embankment is so small when compared with the load of the existing embankment. Consequently, the lateral movements after the additional load is not much when compared to lateral movements due to the embankment load.

The maximum lateral movement in the soft clay subsoil occurred at about 2.5 to 4.0 m below the ground surface, corresponding to the weakest zone of the subsoil layer. The lateral movements during construction and in the post construction surcharge phase were quite considerable. Most of the lateral movements in the subsoil occurred within 50 days from the beginning of the additional surcharge construction, and thereafter, slowed down considerably. The additional surcharge construction lasted for 7 days. The rate of the lateral movements of the wall face slowed down considerably within 90 days after completion of additional surcharge. The lateral movements versus depth before and after additional surcharge are shown in Fig. 17.

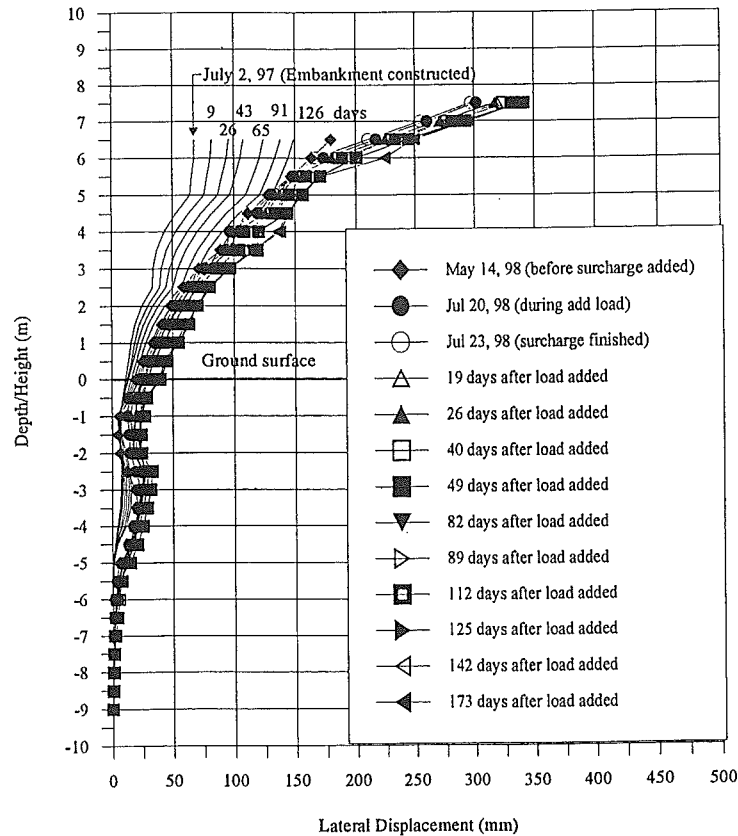


Fig. 17 Lateral Movement From Test Embankment Before and After Additional Surcharge

DISPLACEMENT OF WIRE MESH

The displacement in the wire mesh reinforcements were measured using the high strength wire extensometer. Before surcharge, the measured displacements were found to be continually changing, exactly by the horizontal and vertical movements, and the response of the test embankment to these movements. The maximum displacement for both types of the hexagonal wire mesh reinforcements was observed in the topmost layer (layer 6) while the minimum displacement occurred at the bottom layer (layer 1). Moreover, the maximum displacement measured from high strength wire extensometer agreed well with the maximum lateral movement measured by the inclinometer. Further displacements of hexagonal wire mesh reinforcement measured from the displacement board in the embankment with distance from face of the wall in each layer after additional surcharge applied are shown in Fig. 18. The observed period in the figure was counted from the end of embankment construction.

After 15 days from additional surcharge, it can be observed that the displacement of PVC-coated and zinc-coated are very small in mat 1 and 2 of wire mesh and increasing in the upper mat of reinforcement. The maximum displacement occurred in mat 6. Displacements before and after additional surcharge of PVC-coated reinforcement are similar while the displacement is different in zinc-coated zone in which the failure plane moved toward the wall facing.

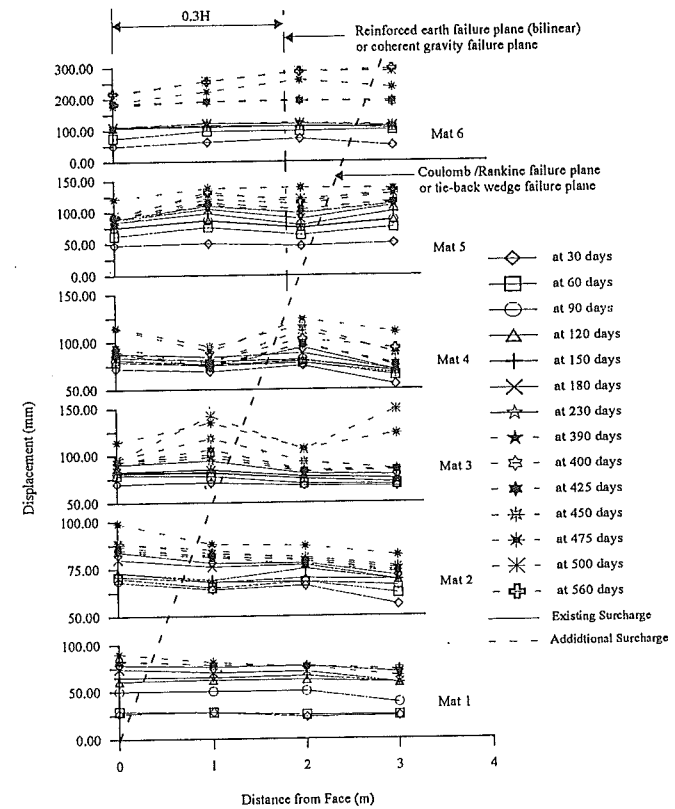


Fig. 18 Displacement of PVC-Coated Reinforcement with Time

In the reinforced soil wall, the maximum tension line can be obtained using both Coulomb/Rankine failure plane or tie-back failure plane and Reinforced earth failure plane or coherent gravity failure plane. The maximum tension line was observed from the plot of displacement board in different periods as shown in Fig. 18. The maximum tension line did not exactly comply with any of the failure planes. However, the maximum tension line is more closer with Coulomb/Rankine failure plane or tie-back wedge failure plane.

PREDICTED SETTLEMENT

The immediate settlement was computed by using Janbu et al (1956) method. This method gives the settlement of 0.017 m due to additional surcharge. In one-dimensional method, the settlement was calculated by dividing the compressible foundation layer into four subsoil layers, and the data from standard oedometer test were used. For the Skempton and Bjerrum (1957) method, the correlation factor, μ is a function of the pore pressure coefficient. Three methods of settlement calculations were used namely: one dimensional, Skempton and Bjerrum, and water content methods. All of these calculations are shown in Tables 2 and 3. Figures 19 and 20 present the settlement prediction by using different C_v values and also show the observed settlement compared with the construction height of reinforced embankment. The calculations using C_v from oedometer test demonstrated that the shape of the predicted settlement curve is steeper than when using C_v from Asaoka's method because the rate of settlement from oedometer test is lower than Asaoka's method (as shown in Tables 4 and 5). The predicted settlement by Asaoka's method yielded closer prediction to the observed settlement. The settlement prediction by using one-dimensional and water content methods are very close together. Most of all, the aforementioned prediction methods overestimated the settlement. The smaller magnitude of the actual observed settlement may be attributed to the presence of the weathered crust acting as raft foundation.

EXTERNAL STABILITY

The external stability of the full scale embankment with additional surcharge in this study was checked, namely: overturning, sliding, and bearing capacity failures with the factors of safety obtained as 17.54, 15.95 and 1.3, respectively.

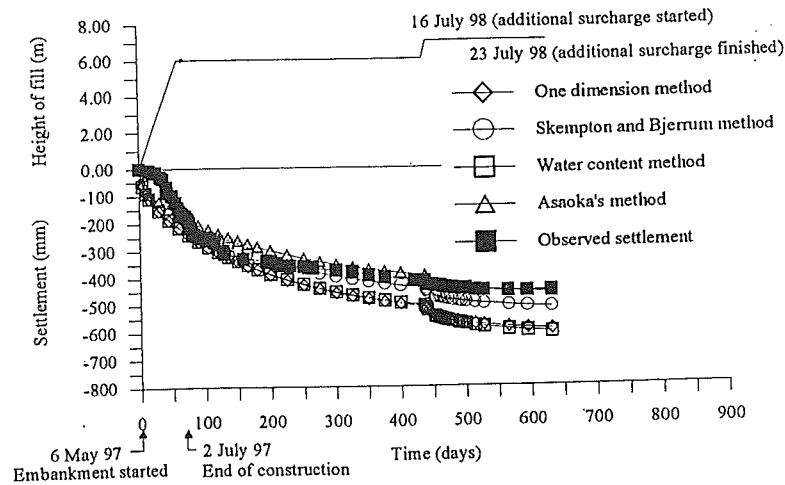


Fig. 19 Observed and Predicted Settlement by Using C_v from Asaoka's Method

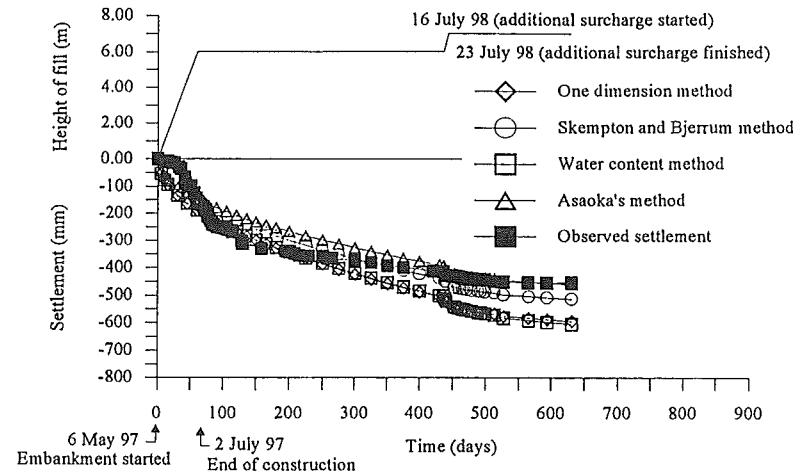


Fig. 20 Observed and Predicted Settlement by Using C_v from Oedometer Test

RELATIONSHIP BETWEEN DISPLACEMENT OF EXTENSOMETER WIRE AND TENSION INDUCED IN THE HEXAGONAL WIRE MESH REINFORCEMENT

From the correlation of laboratory pullout test, the relationship between pullout force, tension from strain gages, and displacement from LVDT can be determined as shown in Fig. 21. The zinc-coated wire mesh has higher stiffness than PVC-coated wire mesh, thus, it was observed that the tension induced in the former is higher than the latter. Moreover, the relationship between displacement and tension in the hexagonal wire mesh shows the same increment for both types of reinforcement.

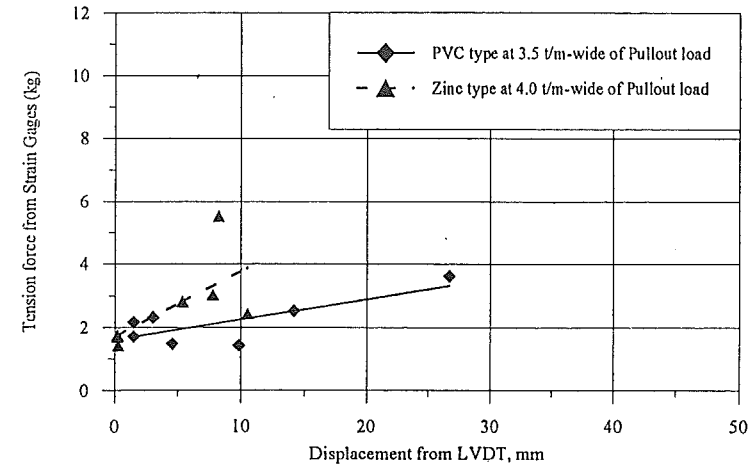


Fig. 21 Relationship Between Tension and LVDT of PVC-Coated and Zinc-Coated Wire Mesh in Silty Sand from Laboratory Test

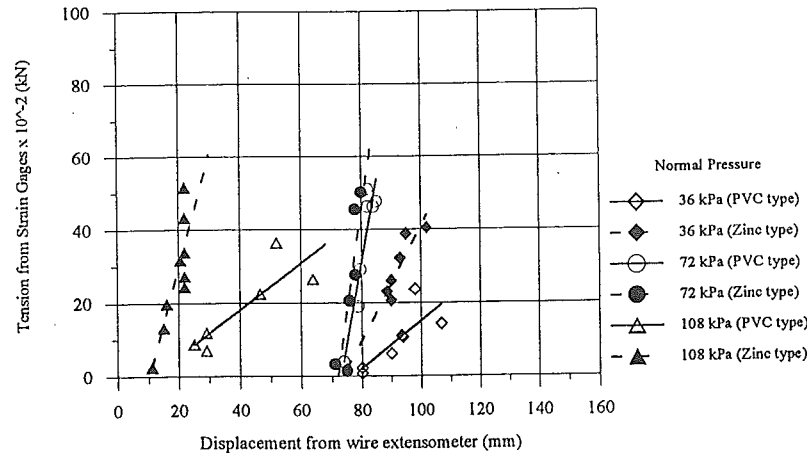


Fig. 22 Relationship Between Force and Displacement of PVC and Zinc-Coated Hexagonal Wire Mesh in Silty Sand from Full Scale Embankment

Figure 22 shows the relationship between the force and the displacement of PVC-coated and zinc-coated from board displacements and field pullout test from full scale embankment. The higher the normal pressure, the lower the displacements. At the same normal pressure, the zinc-coated type shows higher tension than the PVC-coated.

From the comparison between field and laboratory pullout test results, it can be observed that the laboratory pullout test gives higher values due to scale effect. In the laboratory, the pullout tests were done with small scale pullout box in confined condition. Moreover, the facing conditions were not similar, and so were the boundary conditions. However, the compaction and moisture contents can be controlled better in the laboratory test.

CONCLUSIONS

Full scale embankment with hexagonal wire mesh and gabion facing with additional surcharge was constructed to investigate and evaluate the behavior and performance of reinforced embankment. The maximum surface settlement due to additional surcharge was 49 mm observed at the front face of the embankment at 190 days after additional surcharge. The degree of consolidation of subsoil foundation is 80 % after 640 days from the beginning by using C_v from Asaoka's method. The lateral movement that occurred due to additional surcharge is about 7 mm at 173 days corresponding to the zone of the weakest subsoil at about 2.5 m to 4.0 m depth below the general ground surface. The excess pore pressure observed below the embankment at 3.0 m and 6.0 m depths indicate the build up and then dissipation during soil consolidation. The predicted settlement by using Asaoka's method were closer to the observed settlement than the other methods. The maximum tension line which was observed from the wire extensometer connected to the hexagonal wire mesh agreed with the tie-back wedge assumption in the location of the maximum tension line. There is a relationship between displacement and tensions induced in hexagonal wire mesh. The lower the displacement, the lower the tensions induced in the hexagonal wire mesh. Moreover, lower normal pressures induced lower tensions in the hexagonal wire mesh. The zinc-coated hexagonal wires showed higher tensions induced in the wire than PVC-coated in both the field and laboratory tests. The maximum pullout, P_{max} , as a function of normal pressure was developed to an empirical equation for use in the design analysis in the full scale embankment with hexagonal wire mesh reinforcement. The external stability of full scale embankment with hexagonal reinforcement after additional surcharge was checked, namely: the overturning, sliding and bearing capacity with safety obtained as of 17.54, 15.95 and 1.30, respectively.

ACKNOWLEDGEMENT

The authors would like to thank to Mr. S. Khwanpruk and Mr. P. Anujorn for monitoring and providing data and results from their master thesis researches at AIT under Prof. D.T. Bergado. Heartfelt thanks are also extended to Ir. Alan Pun of B.B. Trading (Malaysia) for his generous sponsorship of the research project at AIT.

REFERENCES

- ALFARO, M.C. (1996). Reinforced Soil Wall-Embankment System of Soft Foundation Using Inextensible and Grid Reinforcement. Ph.D. Dissertation, Saga University, Japan.
- ASAOKA, A. (1978). Observational Procedure for Settlement Prediction. *Soils and Foundations*, Vol. 18, No. 4, pp. 87-101.
- BERGADO, D.T., MIR, E.N and PUN, A. (1998a). Hexagonal wire mesh reinforcements with various fill materials including lahar from Mt. Pinatubo, Philippines. *Proceedings Reg. Symp. Infrastructure Planning in Civil Eng'g*, Manila, Philippines, pp. 305-324
- BERGADO, D.T., KABILING, M.B., VOOTTIPTRUEX, P. and PUN, A. (1998b). Pullout capacity of different hexagonal link wires on sandy and volcanic ash landfills. *Proceedings 13th Southeast Asian Geotech. Conf.*, Taipei, Taiwan, pp.259-264
- CASAGRANDE, A. (1936). The determination of the preconsolidation load and its practical significance. *Proceedings 1st Intl. Conf. Soil Mech. Found. Eng'g*, p. 60
- COX, J.B. (1968). A Review of the Engineering Characteristics of the Recent Marine Clays in Southeast Asia. Research Report No. 6, Asian Institute of Technology, Bangkok, Thailand.
- INDRARATNA, B and LASEK, G. (1996). Laboratory evaluation of load-deflection behaviour of clay beams reinforced with galvanised wire netting. *Geotextiles and Geomembranes*, Vol. 14, pp.555-573.
- JANBU, N., BJERRUM, L., and KJAERSLI, B. (1956). Veiledning ved losning av Fundamentertignsoppaver. N.G.I. Publication, No. 16, pp. 93
- KABILING, M.B. (1997). Pullout Capacity of Different Hexagonal Link Wire Mesh Sizes and Configurations on Sandy and Volcanic Ash (Lahar) Backfill. M.Eng. Thesis GE-96-4, Asian Institute of Technology, Bangkok, Thailand.
- KHWANPRUK, S. (1998). Performance of Full Scale Embankment with Hexagonal Wire Mesh Reinforcement and Gabion Facing. M. Eng. Thesis GE-97-11, Asian Institute of Technology, Bangkok, Thailand.
- LO, S.C.R. (1990). Determination of design parameters of a mesh-type soil reinforcement. *Geotechnical Testing Journal*, Vol. 13, No. 4, pp. 343-350
- LO, S.C.R. and LI, S.Q. (1990). Behavior of the Terramesh earth retaining system. *Proceedings 10th Southeast Asian Geotechnical Conference.*, Taipei, Taiwan, pp.83-88
- MACAFERRI (1990). Maccaferri Gabions Manual. Maccaferri South Pacific Pty. Ltd., New South Wales, Australia
- MIR, E.N. (1996). Pullout and Direct Shear Tests of Hexagonal Wire Mesh Reinforcements in Various Fill Materials Including Lahar from Mt. Pinatubo, Philippines. M.Eng. Thesis GE-95-18, Asian Institute of Technology, Bangkok, Thailand.
- MODMOLTIN, C. (1998). Behavior of Hexagonal Wire Mesh Reinforcement in Full Scale Embankment Load and During Pullout. M. Eng. Thesis GE-97-6, Asian Institute of Technology, Bangkok, Thailand.
- SKEMPTON, A.W. and BJERRUM, L. (1957). A contribution to the settlement analysis of foundations on clays. *Geotechnique*, Vol. 7, No. 4, pp. 168-178.

- TEERAWATTANASUK, C.(1997). Interaction and Deformation Behavior of Hexagonal Wire Mesh Reinforcement at Vicinity of Shear Surface on Sand and Volcanic Ash (Lahar) Backfills. M.Eng. Thesis No.GT-96-14, Asian Institute of Technology, Bangkok, Thailand
- VOOTTIPRUEX, P., D.T. BERGADO, C. MODMOLTIN, and S. KHWANPRUK (1998). Deformation characteristics of hexagonal wire mesh reinforcement. *Proceedings of Intl. Symp. On Lowland Technology*, Saga University, Japan
- WONGSAWANON, T. (1998). Interaction Between Hexagonal Wire Mesh Reinforcement and Silty Sand Backfill. M. Eng. Thesis GE-97-14, Asian Institute of Technology, Bangkok, Thailand.

STRESS DISTRIBUTION IN SUBGRADE SOILS AND APPLICATIONS IN THE DESIGN OF FLEXIBLE PAVEMENTS

Y. Qiu¹, N.D. Dennis², and R.P. Elliott³

ABSTRACT

A comprehensive study of stress distribution in highway subgrades of flexible pavements was conducted. A stress-dependent non-linear finite element method (FEM) program, ARKPAVE, was used to generate structural responses of pavements under vehicle loads. The subgrade depth of interest was found to be around 1500 mm. The confining pressure within this depth of interest ranges from 15 to 40 kPa and averages about 20 kPa. This average confining pressure is recommended to be the chamber pressure in triaxial and/or repeated load testing in the evaluation of subgrade soils. The distribution of deviator stress along the subgrade depth was found to be more or less independent of the layer thickness combinations. It is shown that the stress at the top of the subgrade is a better criterion than the vertical resilient strain. This stress was mapped out in accordance with the various thickness selections including full-depth asphalt concrete (AC) pavements which can be readily incorporated into a modern pavement management system. The contours of deviator stress at the top of the subgrade also facilitate the optimum design of flexible pavements as demonstrated in the paper by a design example. This approach advocates the feasibility and promptness of the adoption of rational mechanistic-empirical (M-E) design methods for pavement structures.

INTRODUCTION

Given traffic and environment, subgrade soils govern the succeeding layer combination and thickness selection in the design of pavement structures. Subgrades beneath a pavement also have a controlling influence on how long and how well a pavement performs. The major forms of distress that causes an asphalt pavement to fail are fatigue cracking and surface rutting. The development of both types of distresses is largely controlled by the support the pavement receives from the subgrade when subjected to vehicle loads. The support provided by the subgrade is controlled by the load deformation behavior of the soil, which can be divided into two components:

$$\varepsilon = \varepsilon_r + \varepsilon_p \quad (1)$$

where:

ε	=	load-induced subgrade strain
ε_r	=	resilient (or recoverable) strain
ε_p	=	permanent or residual strain

The pronounced influence of subgrade soils on both distress modes was recognized long ago (Seed et al., 1962). The resilient modulus (defined in Eq. 2) and permanent deformation (or permanent strain) are usually used to characterize the resilient and residual deformation behaviors of subgrades, which in turn are thought to be the direct factors governing the initiation-propagation of fatigue cracking and accumulation of rutting, respectively.

$$M_R = \sigma_d / \varepsilon_r \quad (2)$$

where:

M_R	=	resilient modulus (kPa)
σ_d	=	deviator stress ($\sigma_1 - \sigma_3$) (kPa)

1 Assistant Professor, School of Civil Engineering, Southwest Jiaotong University, Chengdu, 610031, P. R. China

2 Associate Professor, 4190 Bell Engineering Center, Department of Civil Engineering, University of Arkansas, Fayetteville, AR72701, USA.

3 Professor and Head, 4190 Bell Engineering Center, Department of Civil Engineering, University of Arkansas, Fayetteville, AR72701, USA.

Note: Discussion is open until 1 August 2000. This paper is part of the *Geotechnical Engineering Journal*, Vol. 30, No. 3, December 1999. Published by the Southeast Asian Geotechnical Society, ISSN 0046-5828.